Ab initio study of the neutral and anionic alkali and alkaline earth hydroxides: electronic structure and prospects for sympathetic cooling of OH^-

Milaim Kas,[1, a)] Jérôme Loreau,[1] Jacques Liévin,[1] and Nathalie Vaeck[1]
Service de Chimie Quantique et Photophysique (CQP)
Université libre de Bruxelles (ULB), Brussels, Belgium

(Dated: February 3, 2017)

We have performed a systematic *ab initio* study on alkali and alkaline earth hydroxide neutral (MOH) and anionic (MOH^-) species where M = Li, Na, K, Rb, Cs or Be, Mg, Ca, Sr, Ba. The CCSD(T) method using extended basis sets and MDF electron core potentials as been used to study their equilibrium geometries, interaction energies, adiabatic electron affinities and potential energy surfaces. All neutral and anionic species exhibit a linear shape with the exception of BeOH, $BeOH^-$ and $MgOH^-$, for which the equilibrium structure is bent. In the context of sympathetic cooling of OH^- by collision with ultracold alkali and alkaline earth atoms, we investigate the M- OH^- potential energy surfaces and the associative detachment reaction $M+OH^- \rightarrow MOH+e^-$, which is the only energetically allowed reactive channel in the cold regime. We discuss the implication for the sympathetic cooling of OH^- and conclude than Li and K are the best candidates for ultracold buffer gas.

I. INTRODUCTION

Anions play an important role in many different fields of chemistry and physics, from the chemistry in Earth's atmosphere[1] to the study of highly correlated systems[2,3]. In particular, the detection of molecular anions in various astrophysical environments (coma of comets[4], interstellar molecular clouds[5], and extraterrestrial atmospheres[6]), the recent prospects for laser cooling of atomic[7] and molecular[8] anions, and the possibility of using anions for sympathetic cooling of anti-protons[9] are some of the exciting topics which have broadened the interest on the structure and dynamics of molecular anions.

Anionic alkali and alkaline earth hydroxides (MOH^-) are simple molecular anions, and their study can bring new insights into the molecular structure and bonding properties of anions. Neutral alkali and alkaline earth hydroxides (MOH) have been extensively studied both theoretically[10–20] and experimentally[21–35] (see also the reviews of A.Ellis[36] and Gurvitch *et al.*[37]). The interest lies in the general context of molecular structure and the understanding of the M-O bond. The alkali and heavy alkaline earth (Ca, Sr, Ba) hydroxides are known to exhibit a linear equilibrium geometry while lighter alkaline earth hydroxides are either quasi linear (MgOH)[22] or bent (BeOH)[15]. The linear structure is usually explained by the strong ionic character of the alkali and heavy alkaline earth hydroxides while the more covalent character of the BeOH and MgOH molecules favors a bent structure. Moreover, they all exhibit a low energy bending degree of freedom, making the compounds «floppy» upon the bending motion. On the other hand, no information exist on their anion counterparts, with the exception of $RbOH^-$ for which several theoretical studies have been performed in the context of cold chemistry[38–41].

One of the contexts in which the MOH^- anions can play a role is sympathetic cooling of OH^- by collision with ultracold alklali and alkaline earth atoms. Direct laser cooling method are routinely used to reach the utracold regime for neutral and cationic atoms (mostly alkali and alkaline earth) but have so far never been applied to anions even tough some atomic anions such as La^- and Os^- exhibit stable excited electronic states and represent potential candidates for laser cooling[7,42]. The direct laser cooling of molecules is complicated by the lack of closed transition cycles and requires advanced cooling schemes. It has only been successfully applied to a few diatomic molecules such as SrF[43], CaF[44] and YO[45]. Laser cooling strategies have been proposed for diatomic anions[8] such as C_2^- but not yet realized. Sympathetic cooling offers a simpler and more general way to reach the ultracold regime for molecules. The method relies on collisions between cold or ultracold atoms and the target species. Cryogenic helium is widely used as a buffer gas to cool down translational and internal degrees of freedom of various neutral and ionic molecules but the temperature is limited to a few Kelvin. Another possibility is to use laser-cooled atoms as a buffer gas, in which case the experimental setup is usually a combination of a cooling scheme such as a magneto optical trap (MOT) and an ion trap used to confined the target ion. The ability of the ultracold atom to cool the translational and internal degrees of freedom of the target ion will depend on the polarizability of the atom, the mass ratio m_M/m_{OH} and the shape of the potential energy surface (PES) that characterizes the collision. In addition, chemical reactions such as charge transfer or associative detachment may occur in such environments, leading to a loss of the ion if the kinetic energy release is larger than the trap depth or if the ion loses its electric charge. The hydroxyl anion OH^- is one of the simplest and most studied molecular anions. Its behavior in rf traps has been extensively studied[46–48] and photodetachment tomography can be used as a thermometer for the temperature of internal

a) Electronic mail: milakas@ulb.ac.be

degrees of freedom[48] which have been well characterized. The OH^- anion therefore seems to be an ideal candidate for the experimental realization of the sympathetic cooling of anions. The cooling of OH^- by ultracold Rb atoms has been studied experimentally[49], but it was shown that the process is hindered by the associative detachment reaction $Rb + OH^- \rightarrow RbOH + e^-$.

The first objective of the present paper is to investigate the structural properties of the MOH^- anions (where M=Li, Na, K, Rb, Cs, or Be, Mg, Ca, Sr, Ba). We compare these properties to those of the corresponding neutral alkali and alkaline earth hydroxides MOH and we emphasize the differences between the neutral and anionic species. We also discuss the trends along the alkali and alkaline earth series. The second objective is to investigate the prospects for sympathetic cooling of OH^- on the basis of the M-OH^- potential energy surfaces and the $M + OH^- \rightarrow MOH + e^-$ associative detachment reaction.

The paper is structured as follows: in Sec. II we describe the computational method, in Sec. III we investigate the molecular structure and properties of the alkali and alkaline earth anion and neutral hydroxides, and in Sec. IV we discuss the potential energy surfaces, the associative detachment reaction, and the implications for sympathetic cooling.

II. COMPUTATIONAL METHOD

All calculations were performed on the Hydra and Vega clusters of the ULB/VUB computing center using the MOLPRO 2012 package[50]. The coordinates used to describe the molecular species MOH and MOH^- are represented on Figure 1, with the usual Jacobi coordinates: R_M the distance between M and the center of mass of OH, R_{OH} the distance between O and H, and θ the angle between the $\mathbf{R_M}$ and $\mathbf{R_{OH}}$ vectors, and R_{MO} the distance between the M and O atoms. Accordingly, the geometry for $\theta = 0°$ corresponds to the case where the M-O-H atoms are aligned whereas $\theta = 180°$ corresponds to the O-H-M collinear configuration.

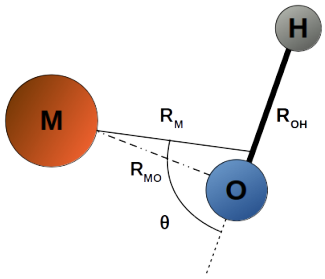

Figure 1. Coordinates defining the MOH anionic and neutral systems.

The coupled cluster level of theory with single, double and perturbative triple excitations (CCSD(T)) as implemented in the MOLPRO program[51] was used for all calculations. The electronic structure of the alkali atoms are $[core](n-1)s^2(n-1)p^6ns^1$ with n corresponding to the highest principal quantum number, while for the alkaline earth atoms the ns orbital is doubly occupied (ns^2). Li and Be are exceptions as they do not have p electrons, and their electronic structures are $1s^22s^1$ and $1s^22s^2$, respectively. In the following, we will refer to the $(n-1)s^2(n-1)p^6$ (or $1s^2$ for Li and Be) electrons as outer core electrons (oc) and the ns^1 or ns^2 electron(s) as valence electrons (val). For the lighter atoms Li, Na, Be, and Mg, the augmented correlation-consistent polarized valence basis set aug-cc-pVnZ (shortened as AVnZ, with n= Q or 5)[52] was used for valence correlation whereas the aug-cc-pwCVnZ core-correlation consistent basis set (shortened AWCVnZ) was used when including the outer core electrons into the correlation treatment. Explicitly treating the outer core electrons allows to account for the outer core-valence correlation. The Dirac-Fock ECPMDF relativistic effective core potentials (ECP) were used for the K, Rb, Cs, Ca, Sr and Ba atoms[53]. These ECPs allow an explicit correlation treatment of the outer core and valence electrons. The corresponding basis sets published alongside the ECPs were used: segmented spdfg functions for Rb, Cs, Sr and Ba atoms, spdf functions for K and spd functions for Ca[53]. For the alkali and alkaline earth atoms, each type of functions has been supplemented by a single even tempered function for which the exponent is determined from the exponents of the last two functions of the previous basis. AVnZ and AWCVnZ basis sets were used for the H and O atoms, respectively. The $1s_O$ orbital was included in the correlation treatment.

III. MOLECULAR PROPERTIES

At linear geometry ($C_{\infty v}$ symmetry), the electronic ground state of the alkali hydroxide anion MOH^- is defined by the $X\,^2\Sigma^+$ term symbol whereas the neutral MOH species is a $X\,^1\Sigma^+$ state. At bent geometries (C_s symmetry), these states correlate to $X\,^2A'$ and $X\,^1A'$, respectively. For the alkaline earth hydroxides, the ground state at linear geometry is $X\,^2\Sigma^+$ for the neutral and $X\,^1\Sigma^+$ for the anion, and $X\,^2A'$ and $X\,^1A'$ states at bent geometries, respectively. We have performed geometry optimizations for all alkali and alkaline earth neutral and anionic species. The neutral alkali and alkaline earth hydroxides exhibit a linear structure with the exception of BeOH. All MOH^- anions are stable (lower in energy than the neutral). Their equilibrium structure is also linear for M=Li,Na, K, Rb, Cs, Ca, Sr and Ba. For $MgOH^-$ and $BeOH^-$, however, the equilibrium structure is predicted to be bent. In the case of Mg and Be hydroxide all three nuclear coordinates variables were optimized, i.e θ, R_{MO} and R_{OH}. For all other species, after making

sure that the equilibrium geometries corresponds to a linear case (by examining the PES near θ=0°), the angle θ was held fixed at 0° and R_{MO} and R_{OH} were optimized. The calculated optimized angle for BeOH, $BeOH^-$ and $MgOH^-$ is 37°, 66° and 50° respectively. Our results for the optimized distances are presented in Table I and Figure 2 along available experimental values for the neutral species.

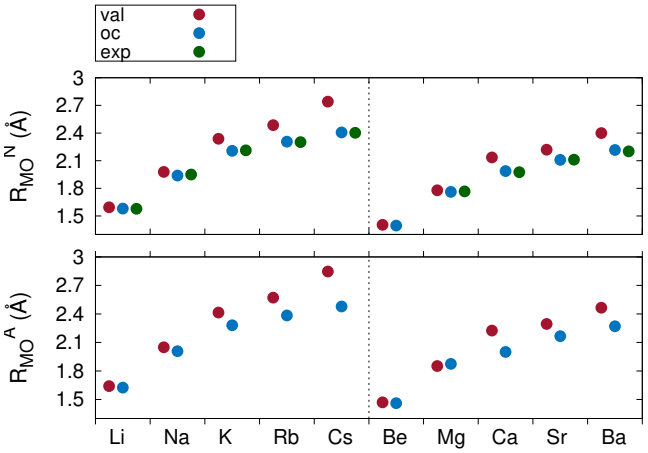

Figure 2. Optimized R_{MO} distance for various alkali and alkaline earth hydroxide anions (upper panel) and neutrals (lower panel). The blue dots corresponds to outer core calculations (oc), red dots corresponds to valence correlation (val) and green dots are experimental values (see Table I for references). The ACVQZ and AWCVQZ basis set were used for the Li, Na, Mg, O and H atoms for val and oc calculations, respectively. See section II for the basis used for the heavier alkali and alkaline earth atoms.

Figure 2 shows the optimized R_{MO} distance for valence and outer core calculations. As can be seen, the R_{MO} equilibrium distance increases with the size of the alkali for both the anionic and neutral species. The equilibrium distances for the anion are slightly larger than for their neutral counterparts, as expected from the weakening effect of the added electron on the bond strength and the more diffuse electronic density of the anion. The largest difference occurs for the Mg hydroxide for which the difference in the R_{MO} distance is 0.11 Å which is due to the bent structure of $MgOH^-$. The inclusion of outer core electrons in the correlation treatment gives results that are closer to experimental values. In particular, the effect of the outer core correlation increases with the size of the M atoms. This is not surprising since the difference in energy between the valence and outer core orbitals decreases with increasing size of M and, therefore, the magnitude of their interaction increases as well. This trend is less marked for the alkaline earth hydroxides and a deviation can be observed for CaOH. This can be attributed

Table I. CCSD(T)/oc optimized R_{MO} and R_{OH} distances (in Å) for the neutral and anion MOH species. The AWCV5Z basis set has been used for O, Be, Li and Mg, AWCVQZ for Na and AV5Z basis set for H. See section II for the basis used for the heavier alkali and alkaline earth atoms. Experimental values are given for the neutral case, when available. All species have a linear equilibrium structure except BeOH, $BeOH^-$ and $MgOH^-$ for which the calculated equilibrium angle θ is 37°, 66° and 50° respectively.

	Anion		Neutral			
	This work		This work		Exp.	
	R_{MO}	R_{OH}	R_{MO}	R_{OH}	R_{MO}	R_{OH}
LiOH	1.623	0.949	1.579	0.948	1.578	0.949[54]
NaOH	2.007	0.953	1.938	0.951	1.95[27]	-
KOH	2.274	0.955	2.202	0.954	2.196	0.960[34]
RbOH	2.380	0.956	2.303	0.955	2.301	0.957[31]
CsOH	2.475	0.957	2.403	0.956	2.391	0.960[30]
BeOH	1.461	0.960	1.395	0.948	-	-
MgOH	1.872	0.956	1.761	0.947	1.767	0.940[22]
CaOH	2.031	0.951	1.977	0.951	1.975	0.957[29]
SrOH	2.161	0.953	2.105	0.952	2.111	0.922[33]
BaOH	2.265	0.955	2.212	0.955	2.201	0.923[26]

to the small basis set used for Ca. Indeed, the optimized companion basis set for the ECP10MDF effective core potential used to describe the 3*s*, 3*p* and 4*s* orbitals of Ca only has [12s,12p,10d] functions, smaller than the basis sets used for the other alkali and alkaline earth atoms. The disagreement is diminished when using 5Z basis set set for O and H (see result in Table I). In table I, both the R_{MO} and R_{OH} distances are presented. The optimized R_{OH} distance does not vary as much as the R_{MO} distance for the different species, yet it also increases with the size of the M atom. The R_{OH} optimized values do not agree as well as the R_{MO} distance with experimental results. This can be explained by the strong anharmonic character of the OH bond. This lead to a large difference between r_e (the geometry at the minimum of the potential energy surface) and r_0 (the expectation value of the ground state vibrational wave function), usually measured in experiments. All neutral species have been known to be linear with the exception of BeOH for which the predicted bent structure has recently been confirmed by a experimental study[15], supported by *ab initio* calculations. Our calculated bond angle agrees with their results. The bent structure is even reinforced in the anionic case, with and increase of θ by 25°. MgOH, which has a quasi linear structure (minimum corresponding to a linear structure but with a very flat PES) becomes bent when adding an excess electron. The obtained barrier to

linearity is around 0.03 eV (242 cm^{-1}) for BeOH, 0.18 eV (1452 cm^{-1}) for $BeOH^-$ and 0.04 eV (323 cm^{-1}) for $MgOH^-$, they all lie below their respective zero-point energy. The linear or bent structures of the different neutral and anionic MOH species can be explained by molecular orbital considerations. Two molecular orbitals need to be considered: the highest occupied molecular orbital (HOMO) of the neutral alkaline earth hydroxide (a a' orbital with mainly ns character) and a the HOMO-2 a' molecular orbital with main contribution from the $2p_x$ atomic orbital of O. We have extracted the Hartree Fock energy of these two orbitals from MOH^- calculations and plotted them as a function of θ. The results are shown in Figure 3 for all investigated species. The

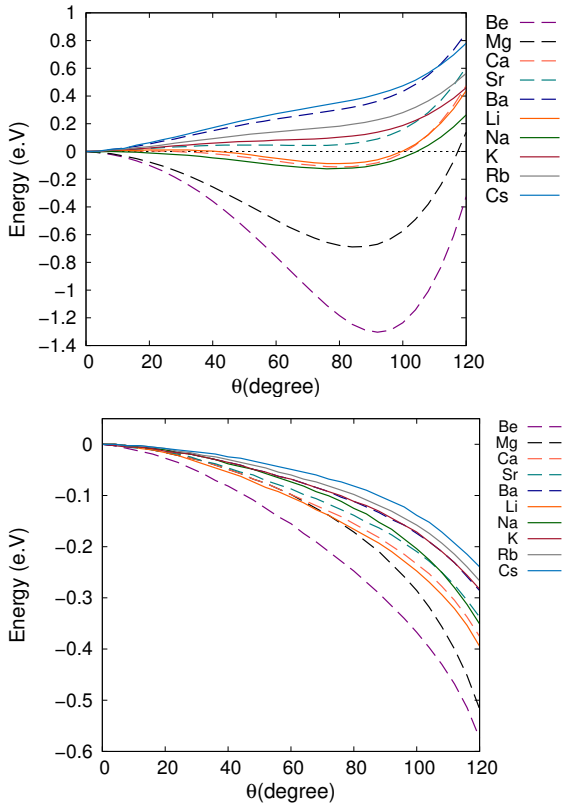

Figure 3. Hartree Fock energies of the HOMO orbital (bottom) and of the HOMO-2 a' molecular orbitals corresponding to the p_x atomic orbital of O (up) for the MOH^- anions as a function of the bending angle θ.

energy of the first orbital (above) decreases with θ for all species, which therefore favors a bent structure. This orbital is unoccupied for the neutral alkali hydroxides, singly occupied for the neutral alkaline earth hydroxides and anionic alkali hydroxides, and doubly occupied for the anionic alkaline earth hydroxides, the influence of the orbital being stronger in the doubly occupied case. The second orbital, doubly occupied in all cases, strongly favors a bent structure for Be and Mg, slightly favors a bent structure for Ca, Na and Li and favors the linear structure for all other species. This HOMO-2 molecular orbital is shown for $BeOH^-$ and $CsOH^-$ in Figure 4. In the case of $CsOH^-$ the molecular orbital exhibit anti-bonding character for the bent structure, which is the opposite for $BeOH^-$ where the bonding character is enhanced at bent geomerties. The behavior of both orbitals with respect to θ allows to explain the bent structure of BeOH, the increase of the bent character for $BeOH^-$ and $MgOH^-$ compared to their neutral counterpart, and the less «floppy» structure of the alkali hydroxides.

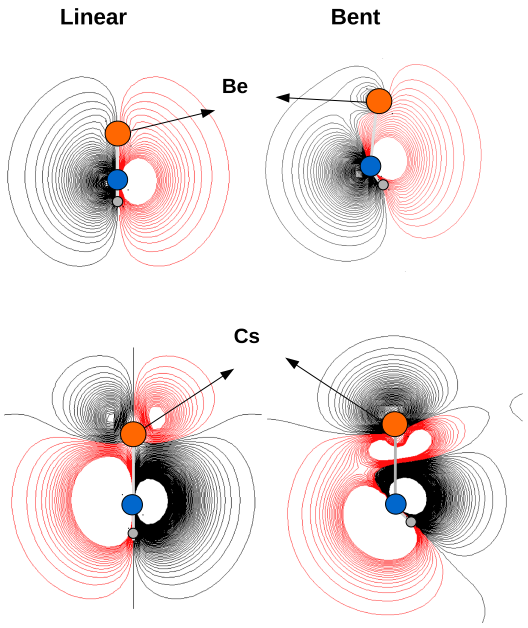

Figure 4. HOMO-2 molecular orbital for the bent and linear structure of $BeOH^-$ (top) and $CsOH^-$ (bellow). Red and black lines corresponds to the positive and negative sign of the electronic wave function. The figure shows the enhanced electronic density for the Be-O bond for bent geometries whereas for $CsOH^-$ the bond exhibit anti-bonding character.

The interaction energies (E_{int}) were also calculated and are shown in Figure 5 and Table II. The E_{int} are obtained by subtracting the energy at dissociation ($M+OH^-$ for the anion and M+OH for the neutral) from the energy of the molecular species at its equilibrium geometry. All calculations were corrected for the harmonic zero point energy (ZPE), obtain at the CCSD(T)/QZ/oc level of theory, and for the basis set superposition error, using the counterpoise method[55].

The interaction energies are very close for all alkali hydroxides with the notable exception of LiOH, for which

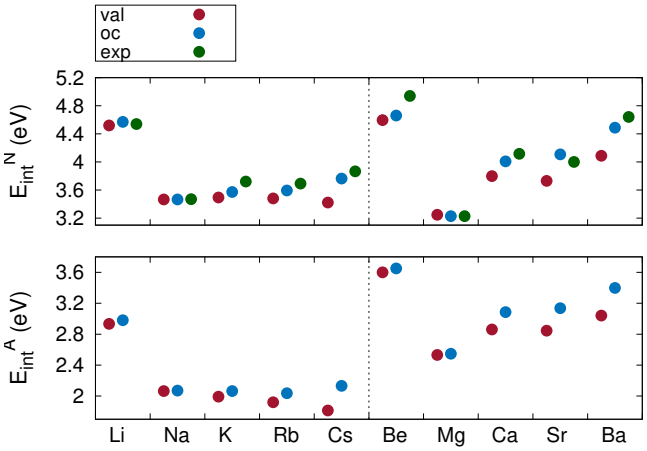

Figure 5. Interaction energy for various neutral (upper panel) and anion (lower panel) alkali and alkaline earth hydroxides. The blue dots corresponds to outer core calculations (oc), red dots corresponds to valence correlation (val) and green dots are experimental values (see Table II for references). The ACVQZ and AWCVQZ basis set were used for the Li, Na, Mg, O and H atoms for val and oc calculations, respectively. See section II for the basis used for the heavier alkali and alkaline earth atoms.

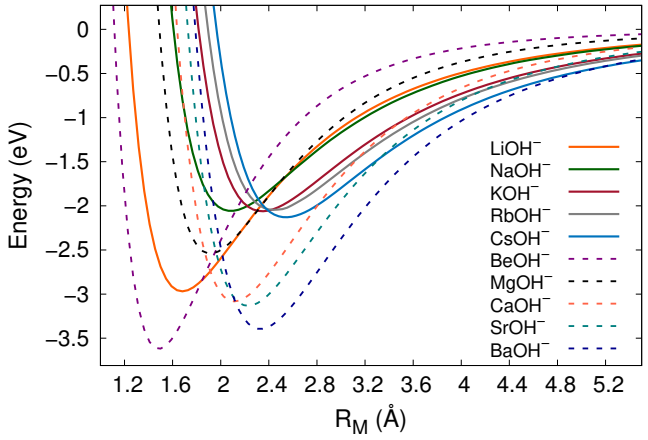

Figure 6. Potential energy curves for the MOH^- anions, where M=Li, Na, K, Rb, Cs and Be, Mg, Ca, Sr, Ba. Curves shown for optimized value of θ (50° for $MgOH^-$, 65° for $BeOH^-$ and 0° for all other anions) with energy relative to the dissociation channel $M+OH^-$. Obtained at the CCSD(T)/oc/QZ level of theory (see section II for computational details). The interatomic R_{OH} distance was held fixed at its CCSD(T)/QZ equilibrium value (0.9643 Å). Solid lines corresponds to alkali hydroxides whereas the dashed lines corresponds to alkaline earth hydroxides.

the interaction is much stronger. An increase in interaction energy is observed for the alkaline earth hydroxides. Similar to the case of Li, the binding energy of the Be hydroxide is significantly larger than for the other alkaline earth hydroxides, for both the neutral and anion. In addition, the alkaline earth hydroxides are predicted to be more stable than the alkali hydroxides. Our conclusion on the effect of the correlation of outer core electrons for the intermolecular distance also applies to the interaction energies, i.e the effect increases with increasing size of the M atom.

Figure 6 shows the potential energy curves of the different MOH^- anions as a function of the distance R_M for the equilibrium value of θ, i.e. bent for $MgOH^-$ and $BeOH^-$ and linear for all other anions. This figure offers a pictorial view of the major differences between the MOH^- species: the variation in equilibrium distance and depth of the interaction well.

For all investigated species, the anion is stable (lower in energy than the neutral) at intermediate and large R_{MO} distances, resulting in a positive electron affinity (EA). Table III shows the adiabatic electron affinities of the alkali and alkaline earth hydroxides. No experimental or theoretical values are available for comparison. The electron affinities of the alkali hydroxides decrease with increasing size of the alkali. A similar trend occurs in the atomic case[61], which is due to the increase of the screening effect of the nucleus for heavier atoms. The identical trends for the atomic and molecular electron affinities can be explained by the nature of the orbital that binds the excess electron: in the atomic as well as in the molecular case, the bonding orbital corresponds to the *ns* valence orbital of the alkali atom. The situation is different for the alkaline earth atomic anions where the excess electron is loosely bound to the excited *np* orbital. This gives rise to small electron affinities (Ca, Sr and Ba)[62] or no stable atomic anions (Be and Mg)[62]. In the molecular case, the closed-shell configuration of the alkaline earth hydroxide stabilizes the anion for which the excess electron is bound to a $n\sigma$ (or a' in the point group C_s) molecular orbital corresponding mainly to the *ns* valence orbital of the alkaline earth atom, as in the case of alkali hydroxides. LiOH and BeOH do not follow the trend, which is probably due to the lack of *p* orbitals. The MOH^- species are therefore valence bound anions with the excess electron bound by the valence shell molecular orbital. The electron affinities of the alkaline earth hydroxides are larger than for the alkali hydroxides even though their dipole moment are much smaller (e.g around 1.47 D for CaOH[63] and 7.4 D for KOH[64]). This implies that classical charge-dipole interaction is not sufficient to explain the interpret the calculated EAs and suggests strong quantum effect and the importance of electron correlation.

Table II. CCSD(T)/oc interaction energies (in eV) for the neutral and anionic MOH species along with experimental values for the neutral. The AWCV5Z basis set has been used for O, Be, Li and Mg, AWCVQZ basis set for Na and AV5Z basis set for H. See section II for the basis used for the heavier alkali and alkaline earth atoms. The corrected harmonic ZPE value is given in parenthesis.

	Anion	Neutral	
	This work	This work	Exp.
LiOH	2.989(2.895)	4.594(4.475)	4.53[0.04][16], 4.54[56], 4.467[57]
NaOH	2.073(2.011)	3.469(3.388)	3.47[0.09][25], 3.548[57], 3.38[56]
KOH	2.074(2.001)	3.599(3.512)	3.721[57], 3.69[0.09][25], 3.53[56]
RbOH	2.047(1.978)	3.621(3.610)	3.692[57], 3.77[0.09][25], 3.61[56]
CsOH	2.143(2.075)	3.885(3.807)	3.866[57], 3.9[0.09][25], 3.95[56]
BeOH	3.668(3.562)	4.692(4.574)	4.94[0.43][58]
MgOH	2.565(2.500)	3.267(3.187)	3.227[0.22][32], 3.59[0.22][58]
CaOH	3.112(3.023)	4.057(3.947)	4.115[0.435][59], 4.332[0.342][59], 4.23[58]
SrOH	3.157(3.078)	4.148(4.050)	4.00[0.17][60], 4.31[0.10][35], 4.47[25], 4.249 ±0.653[59]
BaOH	3.417(3.343)	4.525(4.436)	4.64[0.17][60]

Table III. CCSD(T)/oc adiabatic electron affinities (EA) of the alkali and alkaline earth hydroxides with the AWCVQZ basis set for Li, Be, Na, Mg and O and AVQZ for H. See section II for the basis used for the heavier alkali and alkaline earth atoms. The ZPE correction has been taken into account (calculated at the QZ/oc level).

MOH	EA(eV)	MOH	EA(eV)
LiOH	0.256	BeOH	0.812
NaOH	0.432	MgOH	1.145
KOH	0.304	CaOH	0.881
RbOH	0.259	SrOH	0.844
CsOH	0.181	BaOH	0.714

IV. POTENTIAL ENERGY SURFACES, ASSOCIATIVE DETACHMENT AND IMPLICATIONS FOR SYMPATHETIC COOLING

The feasibility of sympathetic cooling of OH^- using ultracold Rb atoms has been studied by theoretical methods[38–41] and is currently under experimental investigation using an ion-atom hybrid trap. The first experimental results[49] have shown a loss of OH^- from the trap, which was attributed to the associative detachment (AD) reaction $Rb+OH^- \rightarrow RbOH+e^-$. In a previous work[41], we have shown that the rate coefficient strongly depends on the position of the crossing between the neutral and anion potential energy surfaces (PES) which defines the autodetachment region. This crossing occurs in the repulsive part of the PESs at an energy less than 0.5 eV below the Rb + OH^- dissociation limit, indicating that the AD reaction is barrierless and can be expected to be efficient even in the cold regime. However, if the crossing point occurred above the dissociation limit instead, a dramatically smaller rate coefficient would be obtained. On the other hand, the rate coefficient has a weak dependence in the temperature (*i.e.* the collision energy and the rotational distribution of OH^-). The AD reaction limits the prospects of cooling OH^- in collisions with Rb atoms. However, it is worth investigating whether other laser-cooled alkali or alkaline earth atoms offer better perspectives. To this purpose, we have extended our previous work[41] by calculating the M-OH^- PES and the AD reaction rate using a simple Langevin model.

The global potential energy surfaces of all studied anion hydroxide where obtained at the CCSD(T)/oc/QZ level of theory. They share a common shape similar to the $RbOH^-$ PES obtained by Gonzales *et al.*[38], with the exception of $MgOH^-$ and $BeOH^-$ for which the minimum corresponds to a bent structure, as previously discussed. Figure 7 shows the global 2D potential energy surface of $MgOH^-$ and $NaOH^-$. The different PESs differ in the depth of the potential well and the anisotropy.

To estimate the anisotropic character, we have calculated the energy difference between the θ=180° (at optimized R_{MO}) structure and the global minimum for each species. This very simple model allows to qualitatively discuss the anisotropy character of the different PESs. Results are shown in Table IV. The values seems to follow a trend with increasing anisotropy character for decreasing mass. Lighter atoms are more likely to undergo closer encounter with the colliding partner leading to a stronger interac-

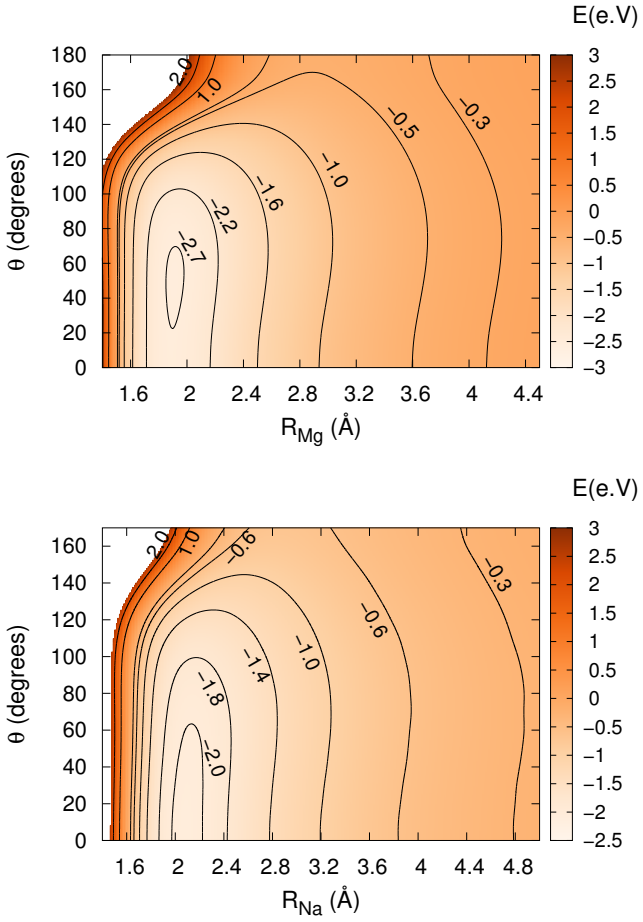

Figure 7. Contour plot of the $MgOH^-$ (left) and $NaOH^-$ (right) 2D potential energy surface. Obtained using the CCSD(T)/oc method with all orbitals correlated except the $1s_{Mg}$ and $1s_{Na}$ and correction for the basis set superposition error. AWCVQZ basis for Mg, Na and O, and AVQZ basis set for H. See section II for the basis used for the heavier alkali and alkaline earth atoms. The interatomic R_{OH} distance was held fixed at its CCSD(T)/oc/QZ equilibrium value (0.9643 Ang).

tion, which can be either favorable (at θ=0° for Li and 65° for Be) or disadvantageous (at θ=180°). Hence, the difference will be less marked for heavier atoms for which the intermolecular distance are larger.

The potential energy surfaces (PES) of the neutral and anion cross in the repulsive region. This crossing point defines the autodetachment region where the anion becomes unstable and can spontaneously autodetach and eject an electron. This will occur for the associative detachment reaction $M+OH^- \rightarrow MOH+e^-$ which is allowed if the anion and neutral curves crosses below the considered energy range. In this case it is the collision energy that induces the detachment of the electron but this may also happen when exciting the vibrational states of MOH^-. The AD reaction produces vibrationally excited MOH and the excess energy is carried away by the ejected electron. The height of the crossing point strongly depends on the system, Figure 8 shows the potential energy curves (PEC) at linear geometry in the repulsive region for the alkali and alkaline earth hydroxides, respectively. A trend can be seen for the alkali hydroxides,

Table IV. CCSD(T)/oc energy difference between global minimum and θ=180° at R_{min} for the anion alkali and alkaline earth hydroxides with the AWCVQ basis set for Li, Be, Na, Mg and O and AVQZ for H. See section II for the basis used for the heavier alkali and alkaline earth atoms.

MOH^-	ΔE (eV)	MOH^-	ΔE (eV)
$LiOH^-$	2.110	$BeOH^-$	3.250
$NaOH^-$	1.420	$MgOH^-$	2.084
KOH^-	1.236	$CaOH^-$	2.272
$RbOH^-$	1.242	$SrOH^-$	2.200
$CsOH^-$	1.396	$BaOH^-$	2.256

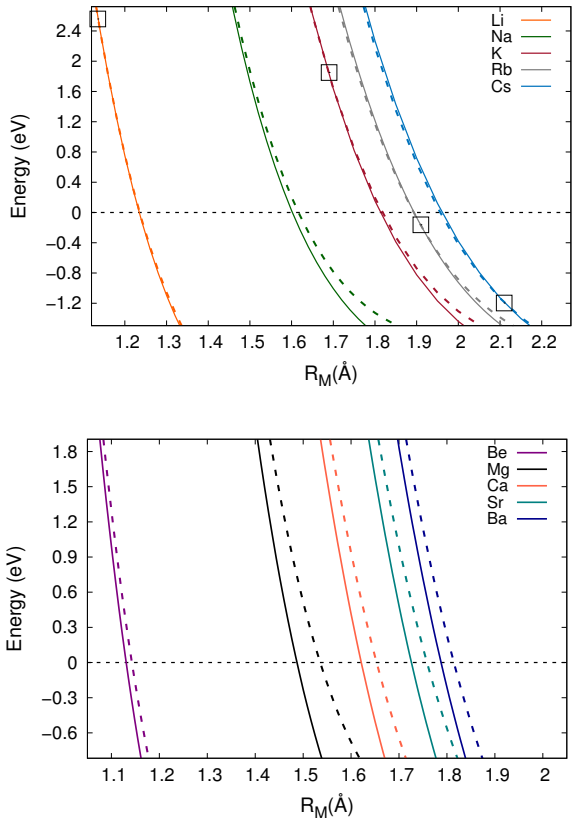

Figure 8. CCSD(T) anion (solid) and neutral (dashed) curves at linear geometry for alkali (left) and alkaline earth (right) hydroxides. The AWCV5Z basis set was used for O, Mg, Li, Na and H, with all electrons correlated except de $1s_{Mg}$ and $1s_{Na}$ orbitals. See section II for the basis used for the heavier alkali and alkaline earth atoms. The crossing point between the curves are indicated by a squares. Energy given relative to the dissociations limit $M+OH^-$.

where the crossing between the anion and neutral PECs occurs lower in energy for heavier alkali. This trend follows the change in electron affinity: the smaller the EA, the lower the crossing. However, the Li hydroxide deviates from the trend and one has to take into account other factors such as the difference between interaction energies of the anion and neutral to explain the position of the crossing point. For the alkaline earth hydroxides, both neutral and anion curves are almost parallel and the crossing occurs much higher in energy. This is also the case in the bent case, suggesting that the curve crossing occurs at very high energy in the entire angular space. The larger electron affinities of the alkaline earth hydroxide explains the higher crossing point. These conclusions support the general idea that anions with higher EA are more stable against detachment process.

As was shown for Rb hydroxide[39,41], the crossing point occurs higher in energy for larger θ values. This is also true for the other hydroxides. This can easily be explained by the increase in energy for both anion and neutral hydroxide in function of θ and by the difference in energy between the neutral and anion PECs. We define $V_c(\theta)$, the height of the crossing point in function of θ. The rate of the associative detachment reaction M + OH^- → MOH + e^- can be obtained from a simple Langevin model which depends upon the height of the crossing point, the collision energy, the Langevin cross section and the ro-vibrational energy of OH^-[39,41]. The AD rate constant for OH^- in its vibrational ground state (v=0) can be expressed as:

$$k_{AD}(T) = \sum_{J=0}^{\infty} \Big(W(J) \int_0^{\infty} f(\varepsilon)\, \sigma_L\, \rho(J, \varepsilon, V_c(\theta))\, d\varepsilon \Big)$$

where $f(\varepsilon)$ is the Maxwell-Boltzmann distribution, σ_L is the Langevin cross section which depends on the mass and the polarizability of the M atom, ρ is the accessible angular space (which depends on $V_c(\theta)$) and ε is the collision energy. The $W(J)$ term accounts for the weight of each rotational state. Figure 9 shows the associative detachment reaction k_{AD} as a function of the height of the crossing point for various temperatures. To obtain the latter, we have used our $V_c(\theta)$ results for $RbOH^-$ and varied $V_c(0)$, the value of the crossing height at θ=0°[41]. By doing so, we assume that the depends on θ of the $V_c(\theta)$ has the same analytical form for all other alkali and alkaline earth atom. We carefully checked that the deviation from this assumption do not significantly affect our conclusions.

One can see that the rate drops dramatically when $V_c(0)$ is above the dissociation limit. However when the crossing point is below the dissociation limit the rate is almost constant with respect to temperature. Note that if the crossing height is below 0 for the entire angular space, the rate constant of the AD reaction will be equal

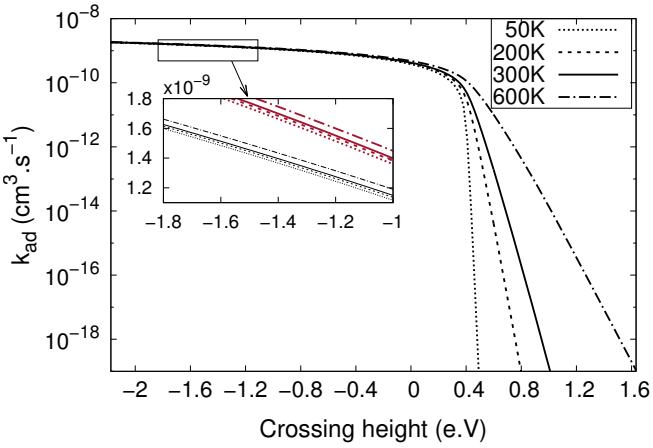

Figure 9. Rate constant of the associative detachment reaction for Rb (black) and Li (red) as a function of the height of the crossing point between anion and neutral curves at linear geometry. Values for several temperatures are plotted. Energy of the crossing point relative to the M+OH^- dissociation limit.

to the Langevin rate. As has been pointed out in our previous work on $RbOH^-$[41], the PECs in the repulsive region are very sensitive to the computational method and basis sets used. To make sure that the choice of the method will not affect our conclusion on the AD reaction, we have calculated the height of the crossing point using different basis sets (AVQZ-AWCVQZ, AV5Z-AWCV5Z, AV6Z when possible and ACWVQZ + extended diffuse functions). We also studied the influence of the R_{OH} bond length on the crossing height. Lithium hydroxide is the most sensitive system with the different calculated crossing height ranging from 0.07 a.u to 0.13 a.u. However, this only affects slightly the conclusion on the AD reaction at low to room temperature since the rate is already below 10^{-17} cm^{3}s^{-1} for a crossing height of 0.03 a.u at 300 K. The same conclusions were reached for all other species. Therefore, the sensitivity of the crossing point will only be relevant for crossings near the threshold energy as for the Rb hydroxide, for which the effect of basis sets and ECPs on the crossing height have already been discussed elsewhere[41]. In addition to the position of the crossing point, the AD rate constant also depends on the Langevin cross section, i.e the mass ratio m_M/m_{OH} and the polarizability of the M atom. The red line on Figure 9 corresponds to k_{AD} obtained using the polarizability and mass of Li. One can see that the difference is only seen for crossing heights below 0 (inset).

Based on the anionic and neutral curve crossings seen on Figure 8 and the behavior of the AD rate constant in function of this crossing height (Figure 9), we can conclude that the AD reaction will only be appreciable for Rb and Cs. The obtained values for the rates are 4.2×10^{-10} cm^{3}s^{-1} and 1.2×10^{-9} cm^{3}s^{-1} at 300K for

Rb and Cs, respectively. The rate weakly depends on the temperature, decreasing to 3.8×10^{-10} cm^3s^{-1} and 1.1×10^{-9} cm^3s^{-1} at 50K, respectively. For comparison, the usual Langevin rate[65] is 4.3×10^{-9} cm^3s^{-1} for Rb-OH^- and 4.7×10^{-9} cm^3s^{-1} for Cs-OH^-. In the context of the experimental study of sympathetic cooling of OH^- with ultracold M atoms, we can make the following conclusions: *i*) The only energetically possible reactive reaction for low to room temperature is the AD reaction. Based on the position of the crossing point between the anion and neutral PES, this reaction should be suppressed for all alkali and alkaline earth atoms except Rb and Cs; *ii*) A low m_M/m_{OH} mass ratio is desirable to avoid heating due to micromotion in radio frequency trap[66], hence the use of lighter M atoms should be preferred; *iii*) The energy of the laser used in the laser cooling scheme of the atom must be lower than the electron affinity of OH (1.82 eV) to avoid photodetachment of OH^-, which leads to a loss of ions. The last condition is only fulfilled by K, Rb and Cs. In the case of the presence of a laser field (e.g use of a MOT), K seems to be the most suitable candidate. In comparison to Rb, the mass ratio is smaller and the loss of OH^- due to the AD reaction will be largely reduced. On the other hand, the relaxation rate should still be as effective[38,40] as for Rb since both species share similar interaction energies and anisotropy characters. Alternatively, one could also use a optical dipole trap instead of a MOT to confine the atoms[67]. In this case the energy of the confining laser is usually lower than the electron affinity of OH[68], suggesting the possibility to use the other mentioned alkali and alkaline earth atoms such as lithium. The latter should be the most suited one since the mass ratio is smaller than 1 while the AD rate should be even smaller than for K. The $LiOH^-$ PES exhibits a deeper well and a stronger anisotropy than for $RbOH^-$. This will affect the elastic and rotational quenching rate constants, and the cooling rates. However, an accurate description of the cooling properties of the Li + OH^- system would require quantum-mechanical nuclear dynamics calculations, which are outside the scope of the present paper.

V. CONCLUSION

A systematic *ab initio* study on the neutral and anion alkali and alkaline earth hydroxides has been performed. Equilibrium parameters, interaction energies and electron affinities have been obtained at the CCSD(T) level of theory. Our results for the neutral species have been compared to experimental values. We found the minimum structure to be linear for all neutral species, with the exception of BeOH, in agreement with the existing literature. To our knowledge, there are no theoretical or experimental studies on the anionic species, and our results constitute the first investigation of the MOH^- molecular anions. All anions are predicted to be linear with the exception of $BeOH^-$ and $MgOH^-$. We tentatively explained this change in the structure by an analysis of the molecular orbitals. Compared to the results for the neutral, the M-O distance are larger for the anions than for the neutrals. This implies a weakening of the chemical bond, which is supported by our results on the interactions energies. The alkaline earth hydroxides have larger electron affinities than alkali hydroxides even though the dipole moment of the latter are much larger. The stability of the alkaline earth hydroxide anions can be explained by their closed shell configuration, suggesting strong electron correlation effects. The potential energy surfaces of the alkali and alkaline earth hydroxide anions exhibit similar shape: a flat potential around the minimum structure ($\theta = 65°$ for $BeOH^-$, 50° for $MgOH^-$ and 0° for the other MOH^- species) and a maximum for the M-H-O conformation. The PESs differ in their depth and anisotropy character.

In the context of sympathetic cooling of OH^- by collisions with ultracold alkali or alkaline earth atoms, we investigated the associative detachment reaction M + OH^- $\rightarrow$ MOH $+e^-$, which is the only energetically accessible reaction in the energy range considered here. Based on the calculated crossing point between the neutral MOH and anion MOH^- PES that defines the autodetachment region, we showed that the AD reaction should only be appreciable for Rb and Cs for which the crossing point occur below the dissociation energy. The usual scheme for sympathetic cooling is based on laser-cooled atoms in a MOT. Many criteria should be fulfilled in order for the cooling process to be efficient: reactive collisions such as AD should be avoided; the laser energy should be lower than the electron affinity of OH to prevent photodetachment; a low mass ratio should be preferred to avoid heating trough coupling with the micromotion in the rf trap; and the elastic cross section should be larger than the inelastic cross section. Based on these considerations, K is the only atom that satisfies all conditions. We note that when using a Paul trap, the mass ratio m_M/m_{OH} should be smaller than 1, but this limitation can be overcome by using higher multipole trap and/or by confining the buffer gas in the region of the trap where micromotion is limited[66].

Alternatively, one could use a optical dipole trap to confine the buffer gas, in which case the energy of the laser is below the electron affinity of OH. This prevents photodetachment and allows a larger choice for the buffer gas. In this case, all alkali and alkaline earth atom except Rb and Cs can be used. Li provides the lowest mass ratio and would therefore seem the most natural choice.

VI. ACKNOWLEDGMENT

M. Kas wishes to thank the HAItrap group of the Heidelberg University and in particular B. Höltkemeier, H. Lopez and Prof. M. Weidemüller, for their hospitality during his stays in Heidelberg and for fruitful discussions. The Fonds National de la Recherche Scientifique de Bel-

gique (FRS-FNRS) is greatly acknowledged for financial support (FRIA grant and IISN 4.4504.10 project). We would also like to thank the ULB/VUB computing center and the CECI team for computational support.

REFERENCES

[1] R. C. Fortenberry, Proc. Int. Astron. Union **9**, 344 (2013).
[2] J. Simons, J. Phys. Chem. A **112**, 6401 (2008).
[3] O. Dulieu and C. Gabbanini, Reports Prog. Phys. **72**, 086401 (2009), 0904.3966.
[4] P. Chaizy, H. Reme, J. Sauvaud, and C. D'Uston, Nature **349**, 393 (1991).
[5] M. McCarthy and C. Gottlieb, Astrophys. , 6 (2006).
[6] V. Vuitton, P. Lavvas, R. Yelle, M. Galand, A. Wellbrock, G. Lewis, A. Coates, and J.-E. Wahlund, Planet. Space Sci. **57**, 1558 (2009).
[7] C. W. Walter, N. D. Gibson, D. J. Matyas, C. Crocker, K. A. Dungan, B. R. Matola, and J. Rohlén, Phys. Rev. Lett. **113**, 063001 (2014).
[8] P. Yzombard, M. Hamamda, S. Gerber, M. Doser, and D. Comparat, Phys. Rev. Lett. **114**, 213001 (2015), 1506.06505.
[9] A. Kellerbauer and J. Walz, New J. Phys. **8**, 45 (2006).
[10] C. W. Bauschlicher, S. R. Langhoff, and H. Partridge, J. Chem. Phys. **84**, 901 (1986).
[11] J. Koput, S. Carter, K. a. Peterson, and G. Theodorakopoulos, J. Chem. Phys. **117**, 1529 (2002).
[12] J. Koput and K. A. Peterson, J. Phys. Chem. A **106**, 9595 (2002).
[13] E. P. F. Lee and T. G. Wright, J. Phys. Chem. A **107**, 5233 (2003).
[14] E. P. F. Lee and T. G. Wright, J. Phys. Chem. A **106**, 8903 (2002).
[15] K. J. Mascaritolo, J. M. Merritt, M. C. Heaven, and P. Jensen, J. Phys. Chem. A **117**, 13654 (2013).
[16] D. McNaughton, L. M. Tack, B. Kleibömer, and P. D. Godfrey, Struct. Chem. **5**, 313 (1994).
[17] C. M. Taylor, R. K. Chaudhuri, and K. F. Freed, J. Chem. Phys. **122**, 044317 (2005).
[18] G. Theodorakopoulos, I. D. Petsalakis, and I. P. Hamilton, J. Chem. Phys. **111**, 10484 (1999).
[19] G. Theodorakopoulos, I. D. Petsalakis, H.-P. Liebermann, R. J. Buenker, and J. Koput, J. Chem. Phys. **117**, 4810 (2002).
[20] M. Vasiliu, D. Feller, J. L. Gole, and D. A. Dixon, J. Phys. Chem. A **114**, 9349 (2010).
[21] N. Acquista, J. Chem. Phys. **51**, 2911 (1969).
[22] A. J. Apponi, M. A. Anderson, and L. M. Ziurys, J. Chem. Phys. **111**, 10919 (1999).
[23] C. Brazier and P. Bernath, J. Mol. Spectrosc. **114**, 163 (1985).
[24] P. Bunker, M. Kolbuszewski, P. Jensen, M. Brumm, M. Anderson, W. Barclay, L. Ziurys, Y. Ni, and D. O. Harris, Chem. Phys. Lett. **239**, 217 (1995).
[25] D. H. Cotton and D. R. Jenkins, Trans. Faraday Soc. **65**, 1537 (1969).
[26] S. Kinsey-Nielsen, C. R. Brazier, and P. F. Bernath, J. Chem. Phys. **84**, 698 (1986).
[27] P. Kuijpers, T. Törring, and A. Dymanus, Zeitschrift fur Naturforsch. - Sect. A J. Phys. Sci. **30**, 1256 (1975).
[28] M. Li and J. a. Coxon, J. Chem. Phys. **104**, 4961 (1996).
[29] M. Li and J. a. Coxon, J. Chem. Phys. **102**, 2663 (1995).
[30] D. R. Lide, J. Chem. Phys. **46**, 4768 (1967).
[31] C. Matsumura, J. Chem. Phys. **50**, 71 (1969).
[32] E. Murad, Chem. Phys. Lett. **72**, 295 (1980).
[33] J. Nakagawa, R. F. Wormsbecher, and D. O. Harris, J. Mol. Spectrosc. **97**, 37 (1983).
[34] E. F. Pearson, B. P. Winnewisser, and M. B. Trueblood, Zeitschrift für Naturforsch. A **31**, 1259 (1976).
[35] J. van der Hurk, T. Hollander, and C. Alkemade, J. Quant. Spectrosc. Radiat. Transf. **14**, 1167 (1974).
[36] A. M. Ellis, Int. Rev. Phys. Chem. **20**, 551 (2001).
[37] L. V. Gurvich, G. a. Bergman, L. N. Gorokhov, V. S. Iorish, V. Y. Leonidov, and V. S. Yungman, J. Phys. Chem. Ref. Data **25**, 1211 (1996).
[38] L. Gonzalez-Sanchez, M. Tacconi, E. Bodo, and F. a. Gianturco, Eur. Phys. J. D **49**, 85 (2008).
[39] J. N. Byrd, H. H. Michels, J. A. Montgomery, and R. Côté, Phys. Rev. A **88**, 032710 (2013).
[40] L. González-Sánchez, F. Carelli, F. Gianturco, and R. Wester, Chem. Phys. **462**, 111 (2015).
[41] M. Kas, J. Loreau, J. Liévin, and N. Vaeck, J. Chem. Phys. **144**, 204306 (2016).
[42] S. M. O'Malley and D. R. Beck, Phys. Rev. A **81**, 032503 (2010).
[43] E. S. Shuman, J. F. Barry, and D. DeMille, Nature **467**, 820 (2010).
[44] V. Zhelyazkova, A. Cournol, T. E. Wall, A. Matsushima, J. J. Hudson, E. A. Hinds, M. R. Tarbutt, and B. E. Sauer, Phys. Rev. A **89**, 053416 (2014).
[45] M. T. Hummon, M. Yeo, B. K. Stuhl, A. L. Collopy, Y. Xia, and J. Ye, Phys. Rev. Lett. **110**, 143001 (2013).
[46] J. Mikosch, U. Frühling, S. Trippel, R. Otto, P. Hlavenka, D. Schwalm, M. Weidemüller, and R. Wester, Phys. Rev. A **78**, 023402 (2008).
[47] S. Trippel, J. Mikosch, R. Berhane, R. Otto, M. Weidemüller, and R. Wester, Phys. Rev. Lett. **97**, 193003 (2006), 0607248v2.
[48] P. Hlavenka, R. Otto, S. Trippel, J. Mikosch, M. Weidemüller, and R. Wester, J. Chem. Phys. **130**, 061105 (2009).
[49] J. Deiglmayr, A. Göritz, T. Best, M. Weidemüller, and R. Wester, Phys. Rev. A **86**, 043438 (2012).
[50] H.-J. Werner, P. J. Knowles, G. Knizia, F. R. Manby, M. Schütz, P. Celani, T. Korona, R. Lindh, A. Mitrushenkov, G. Rauhut, K. R. Shamasundar, T. B. Adler, R. D. Amos, A. Bernhardsson, A. Berning, D. L. Cooper, M. J. O. Deegan, A. J. Dobbyn, F. Eckert, E. Goll, C. Hampel, A. Hesselmann, G. Hetzer, T. Hrenar, G. Jansen, C. Köppl, Y. Liu, A. W. Lloyd, R. A. Mata, A. J. May, S. J. McNicholas, W. Meyer, M. E. Mura, A. Nicklass, D. P. O'Neill, P. Palmieri, D. Peng, K. Pflüger, R. Pitzer, M. Reiher, T. Shiozaki, H. Stoll, A. J. Stone, R. Tarroni, T. Thorsteinsson, and M. Wang, "MOLPRO, version 2012.1, a package of ab initio programs," (2012).
[51] C. Hampel, K. a. Peterson, and H.-J. Werner, Chem. Phys. Lett. **190**, 1 (1992).
[52] T. H. Dunning, J. Chem. Phys. **90**, 1007 (1989).
[53] F. Weigend and A. Baldes, J. Chem. Phys. **133**, 174102 (2010).
[54] K. J. Higgins, S. M. Freund, W. Klemperer, A. J. Apponi, and L. M. Ziurys, J. Chem. Phys. **121**, 11715 (2004).
[55] S. Boys and F. Bernardi, Mol. Phys. **19**, 553 (1970).
[56] D. E. Jensen, J. Phys. Chem. **74**, 207 (1970).
[57] W. Haynes, *CRC Handbook of Chemistry and Physics* (CRC Press, 2012).
[58] M. Chase, J. Curnatt, R. McDonald, and A. Syverud, J. Phys Chem. Ref. Data **7**, 793 (1978).
[59] D. Darwent, *Bond Dissociation Energies in Simple Molecules*, nbsds-nbs ed. (Washington, DC, 1970).
[60] E. Murad, J. Chem. Phys. **75**, 4080 (1981).
[61] J. C. Rienstra-Kiracofe, G. S. Tschumper, H. F. Schaefer, S. Nandi, and G. B. Ellison, Chem. Rev. **102**, 231 (2002).
[62] P. Fuentealba, A. Savin, H. Stoll, and H. Preuss, Phys. Rev. A **41**, 1238 (1990).
[63] T. C. Steimle, D. a. Fletcher, K. Y. Jung, and C. T. Scurlock, J. Chem. Phys. **96**, 2556 (1992).
[64] J. Cederberg, D. Olson, D. Rioux, T. Dillemuth, B. Borovsky, J. Larson, S. Cheah, M. Carlson, and M. Stohler, J. Chem. Phys. **105**, 3361 (1996).
[65] P. Langevin, P. Ann. Chem. Phys. **5**, 245 (1905).
[66] B. Höltkemeier, P. Weckesser, H. López-Carrera, and M. Weidemüller, Phys. Rev. Lett. **116**, 233003 (2016).
[67] R. Grimm, M. Weidemüller, and Y. B. Ovchinnikov, AAMOP **42**, 95, 9902072.

[68] A. Mosk, S. Jochim, H. Moritz, T. Elsässer, M. Weidemüller, and R. Grimm, Opt. Lett. **26**, 1837 (2001), 0105009.